

## Supporting information

# Bimetallic metal-organic frameworks for the tumor inhibition via combined photothermal-immunotherapy

Anning Li,<sup>a,b</sup> Ning Wang,<sup>a</sup> Yuxuan Song,<sup>a</sup> Haifeng Sun,<sup>a</sup> Jiwei Cui,<sup>a</sup> Guiqiang Zhang<sup>\*a,c</sup> and Qun Yu<sup>\*a</sup>

<sup>a</sup>Key Laboratory of Colloid and Interface Chemistry of the Ministry of Education, School of Chemistry and Chemical Engineering, Shandong University, Jinan, Shandong 250100, China.

<sup>b</sup>Department of Radiology, Qilu Hospital, Cheeloo College of Medicine, Shandong University, Jinan, Shandong 250012, China

<sup>c</sup>Science and Technology Innovation Center, Shandong First Medical University & Shandong Academy of Medical Sciences, Jinan, Shandong 250117, China.

E-mail: gqzhang2018@sdu.edu.cn, qunyu@sdu.edu.cn

## **EXPERIMENTAL SECTION**

### **Materials**

The 8-arm-PEG-OH (40 kDa) was purchased from SINOPEG (China). Indocyanine green (ICG) and methylthiazolyldiphenyl-tetrazolium bromide (MTT) were bought from Sigma-Aldrich (China). RPMI 1640 cell culture medium, fetal bovine serum (FBS), penicillin-streptomycin solution, and trypsin-EDTA solution were purchased from Biological Industries Science & Technology Co. Ltd. (China). Antibody for calreticulin (CRT) was obtained from Rockland Inc. (USA). Hoechst 33342 and wheat germ agglutinin Alexa Fluor 488 conjugate (WGA-AF488) were purchased from Thermo Fisher Scientific (China). All fluorochrome-conjugated anti-mouse antibodies (anti-CD11c, anti-CD80, anti-CD86, anti-CD3, anti-CD4, anti-CD8, anti-CD44 and anti-CD62L) for flow cytometry were purchased from BioLegend (USA) and eBioscience (USA), respectively.

### **Preparation of NPs**

To prepare ICG@ZIF8 NPs, ICG (1 mg) and 8-arm-PEG-OH (10 mg) were dissolved in 2 mL of aqueous solution containing 2-Methylimidazole (2-MIM, 160 mM) and subsequently mixed with 2 mL of  $\text{Zn}(\text{NO}_3)_2 \cdot 6\text{H}_2\text{O}$  (40 mM) solution in water, followed by vigorous stirring at 25 °C for 40 min. Then, the products were collected by centrifugation (7,000g, 5 min) and washed with water and methanol three times. The ICG@ZIF8(Al) NPs were prepared in a similar method for the ICG@ZIF8 NPs. The only difference was that the  $\text{Zn}(\text{NO}_3)_2$  solution containing 8 mM  $\text{AlCl}_3$  was used. The amount of ICG encapsulated into the NPs was analyzed by Ultraviolet-visible (UV-Vis, Shimadzu UV-2600, Japan) spectrophotometry at 780 nm.

### **Characterization**

Hydrodynamic diameter of NPs was measured using a Malvern Zetasizer (Nano ZS90, UK).

The morphology of NPs was observed by transmission electron microscopy (TEM, JEOL JEM-1400, Japan) operating at 120 kV and scanning electron microscopy (SEM, Zeiss G300, Germany). The NP suspension was then examined by using a UV-Vis spectrophotometer and fluorescence spectrophotometer.

### ***In vitro* photothermal evaluation**

The photothermal properties of ICG@ZIF8(Al) NPs at different ICG concentrations (0, 15, 25, 30  $\mu\text{g mL}^{-1}$ ) were investigated under 808 nm laser irradiation ( $1 \text{ W cm}^{-2}$ ) for 5 min by using an infrared camera. The photothermal stability was also evaluated by recording the temperature changes of ICG@ZIF8(Al) NPs and free ICG solution under 808 nm laser irradiation for three laser on/off cycles.

### **Cell uptake**

4T1 cells ( $10^5$  cells per well) were cultured in 24-well plates and then incubated with ICG@ZIF8(Al) NPs for different time intervals (2, 4, 6, 12 h). Cells were then washed three times with PBS and detached for intracellular fluorescence detection using a flow cytometer (ACEA, Novo Cyte 3009, USA).

### **Cytotoxicity**

Cell viabilities of ICG@ZIF8(Al) NPs were analyzed by a MTT assay. Briefly, 4T1 cells ( $10^4$  cells per well) were incubated in 96-well plates with different concentrations of ICG@ZIF8(Al) NPs for 12 h. Cells were washed twice and irradiated with and without 808 nm laser ( $1 \text{ W cm}^{-2}$ ) for 5 min, followed by 12 h incubation. Then, the cell medium was removed and MTT solution was added. The formed formazan crystals dissolved in DMSO was measured at 570 nm using a Tecan microplate reader (Spark 10M, Austria).

### **Live/dead assay**

4T1 cells ( $10^5$  cells per well) were incubated in 24-well plates and incubated with ICG@ZIF8 or ICG@ZIF8(AI) NPs for 12 h. Then, the cells were washed twice and irradiated with and without 808 nm laser ( $1 \text{ W cm}^{-2}$ ) for 5 min. After 2 h incubation, the medium was replaced with 500  $\mu\text{L}$  of PBS containing calcein (2  $\mu\text{M}$ ) and propidium iodide (PI, 4  $\mu\text{M}$ ). Fluorescence images were acquired using an inverted fluorescence microscope.

### **CRT expression**

To observe the surface expression of CRT, 4T1 cells ( $10^5$  cells  $\text{mL}^{-1}$ ) in confocal dishes (Cellvis, Mountain View, CA, USA) were incubated with ICG@ZIF8 or ICG@ZIF8(AI) NPs at an equivalent ICG concentration for 12 h. The cells were subsequently irradiated with 808 nm laser ( $1 \text{ W cm}^{-2}$ ) for 5 min and fixed in 4% paraformaldehyde for 10 min. The cells were then incubated with primary antibody and Alexa 488-conjugated monoclonal secondary antibody for 30 min. Finally, confocal laser scanning microscopy (CLSM) images of CRT expression were obtained by a Leica confocal microscope (TCP SP8 STED 3X, Germany). The expression of CRT was also examined by flow cytometry.

### ***In vitro* analysis of DC maturation**

Bone marrow-derived DCs (BMDCs) were generated by culturing bone marrow cells of C57BL/6 mice in RPMI 1640 medium supplemented with 10% FBS, 20  $\text{ng mL}^{-1}$  of murine GM-CSF and 10  $\text{ng mL}^{-1}$  of murine IL-4. Cells were incubated at 37  $^\circ\text{C}$  supplied with 5%  $\text{CO}_2$ . On day 3, the fresh medium was replenished. On day 6, BMDCs were cocultured with 4T1 cells pretreated with ICG@ZIF8 or ICG@ZIF8(AI) NPs. After 24 h incubation, BMDCs were stained with anti-CD11c and anti-CD80 or anti-CD11c and anti-CD86. The expression of CD11c, CD80, and CD86 was detected by flow cytometry.

### **Inhibition of primary tumor**

Females Balb/c mice were purchased from Vital River Laboratory Animal Technology Co.

Ltd (China). All of the *in vivo* studies were conducted following the regulations of the Animal Ethics Review of Shandong University and the Health Guide for the Care and Use of Laboratory Animals of National Institutes in accordance with the 3R principles of animal experimentation with Reduction, Replacement, and Refinement.

To inoculate the primary tumor,  $1 \times 10^6$  4T1 cells in PBS were subcutaneously injected into the right flank of each mouse. Tumor volume was calculated by  $V = 1/2 \times a \times b^2$ , where a and b represented the tumor length and width, respectively. When the tumor volume was about 100 mm<sup>3</sup>, 4T1 tumor-bearing BALB/c mice were randomly divided into five groups (n=6), i.e., PBS, ICG@ZIF8, ICG@ZIF8 + Laser, ICG@ZIF8(AI), and ICG@ZIF8(AI) + Laser group. On day 0, the mice of each group were intratumorally injected with therapeutics (equivalent ICG dose of 2 mg kg<sup>-1</sup>). At 2 h postinjection, tumors were radiated by 808 nm laser (1 W cm<sup>-2</sup>) for 10 min. Tumor volume and body weight of the mice were monitored every two days. At 14 days after the injection of therapeutics, tumor, heart, lung, liver, and kidneys were separated and weighed. After hematoxylin and eosin (HE) staining, the organ sections were collected for histopathological analysis.

### **DC maturation *in vivo***

To investigate the DC maturation, the inguinal lymph nodes (LNs) of 4T1 tumor-bearing mice treated with different therapeutics were harvested. The DC maturation was examined by flow cytometry.

### **Activation of T lymphocytes in spleen**

At 14 days postinjection, spleen lymphocytes were separated and resuspended with RPMI-1640 complete medium. The lymphocytes were stained with APC-labelled monoclonal antibody against CD3, FITC-labelled monoclonal antibody against CD4, and PE-labelled monoclonal antibody against CD8 (1:1000 dilution) at 4 °C for 45 min. After incubation, the

cells were washed and collected for the detection of CD3<sup>+</sup>CD4<sup>+</sup> and CD3<sup>+</sup>CD8<sup>+</sup> using flow cytometry. To investigate effector memory T cells, the lymphocytes were labelled with anti-CD3, anti-CD8, anti-CD44, and anti-CD62L, followed by the analysis with flow cytometry.

### **Inhibition of rechallenged tumor**

To assess the immune memory response, mice received the same treatments as described in primary tumor model. At 8 days post therapeutics injection (primary tumors almost eliminated), the second tumor was inoculated in the left flank of each mouse as a rechallenged tumor. Tumor volume and body weight of the mice were monitored every 2 days.

### **Intratumoral infiltration of T lymphocytes**

To examine the intratumoral infiltration of CD4 and CD8 T lymphocytes, the second tumors were isolated and digested in the solution of 1 mg mL<sup>-1</sup> collagenase. The single cell suspension was stained with antibodies (anti-CD3, anti-CD4, and anti-CD8) and measured by flow cytometry.

### **Statistical analysis**

Data are presented as mean  $\pm$  SD. A two-tailed Student's *t*-test was performed for the comparison between two groups and one-way ANOVA for multiple group analysis. The *P* value < 0.05 was considered as significant. All data were analyzed using SPSS software (Version 13.0, USA).

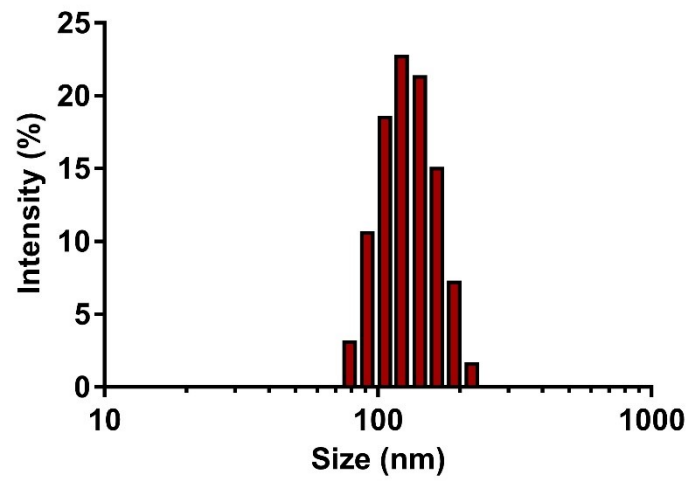


**Figure S1.** Hydrodynamic size distribution of ICG@ZIF8(Al) NPs measured by DLS.

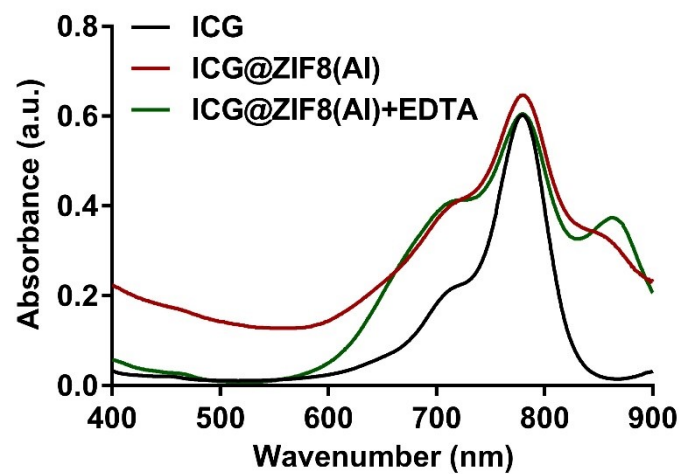


**Figure S2.** UV-Vis absorbance spectra of ICG and ICG@ZIF8(Al) NPs in the presence and absence of ethylenediaminetetraacetic acid (EDTA).

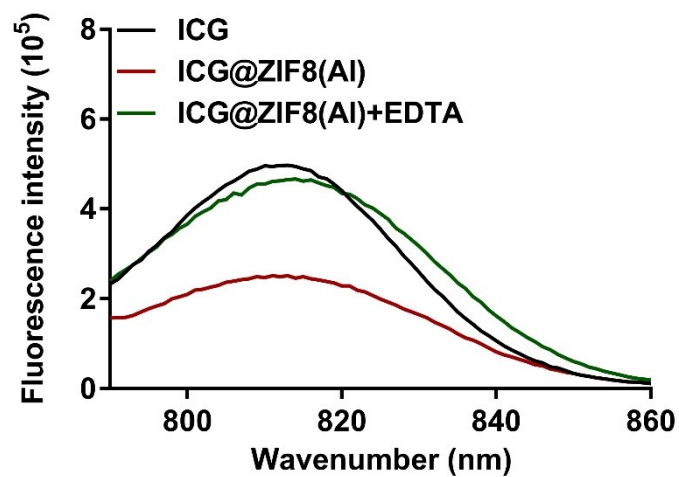


**Figure S3.** Fluorescence spectra of ICG and ICG@ZIF8(Al) NPs in the presence and absence of EDTA.

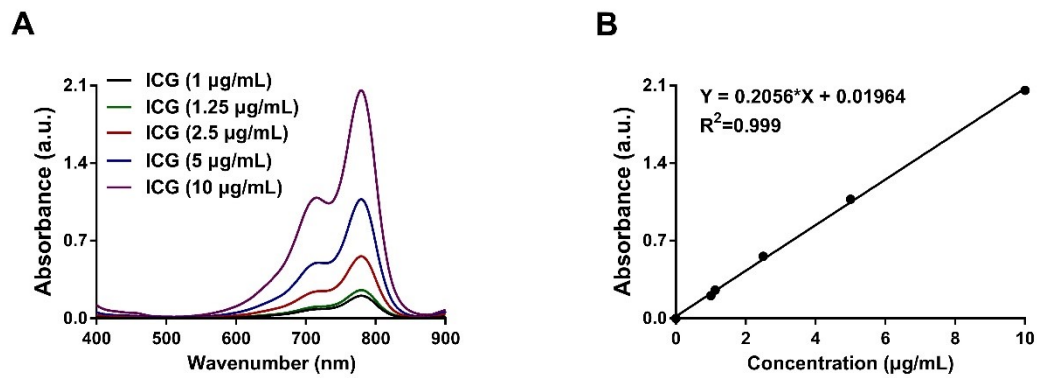
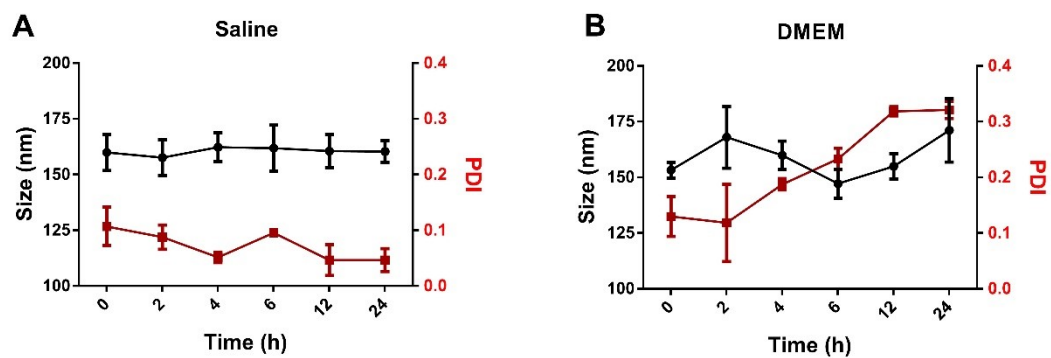
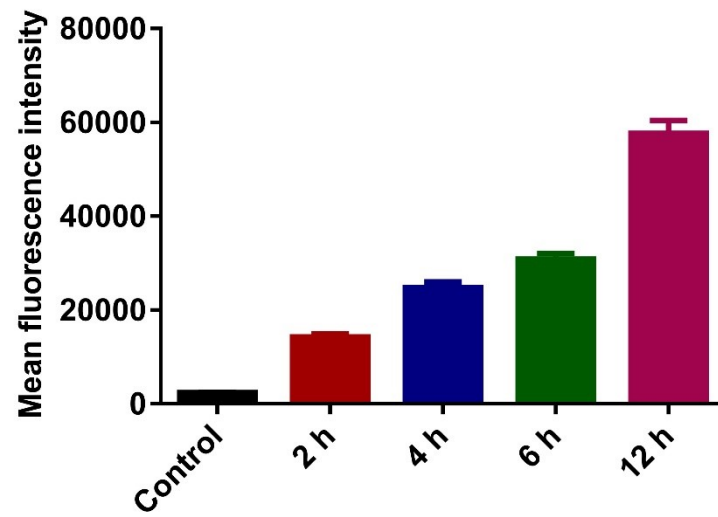


Figure S4. UV-Vis absorbance spectra (A) and standard curve (B) of ICG.



**Figure S5.** Colloidal stability of ICG@ZIF8(Al) NPs in (A) saline and (B) Dulbecco's-modified Eagle's complete medium (DMEM).



**Figure S6.** Cell uptake after incubation with ICG@ZIF8(Al) NPs over different times. Data are represented as the means  $\pm$  SD (n=3).

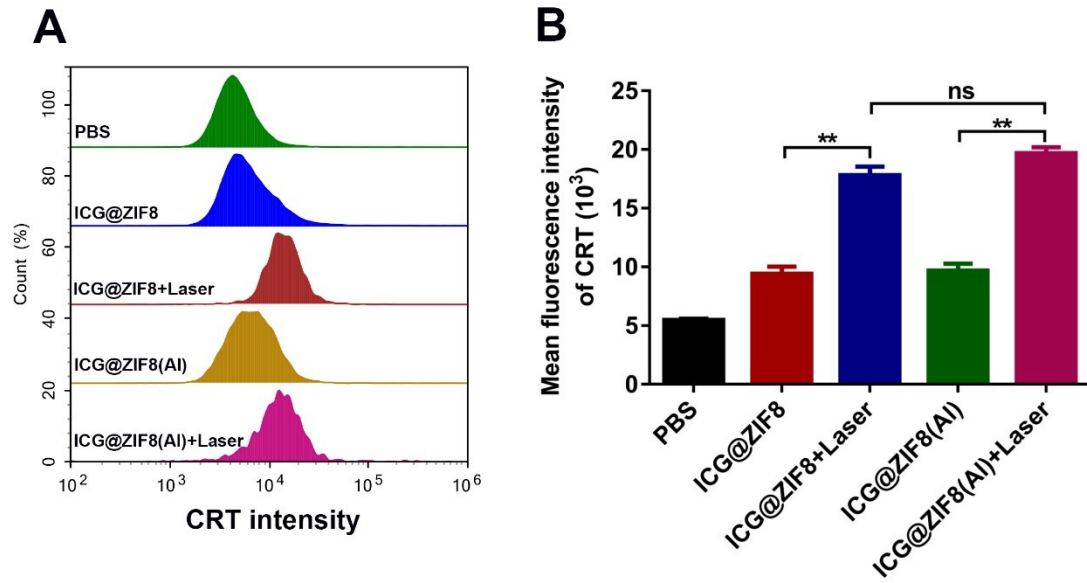


**Figure S7.** Flow cytometry analysis (A) and statistical data (B) of CRT expression in 4T1 cells after incubation with free ICG@ZIF8 or ICG@ZIF8(AI) NPs in the absence and presence of laser radiation.

Data are represented as the means  $\pm$  SD (n=3). \*\* $P < 0.01$ .

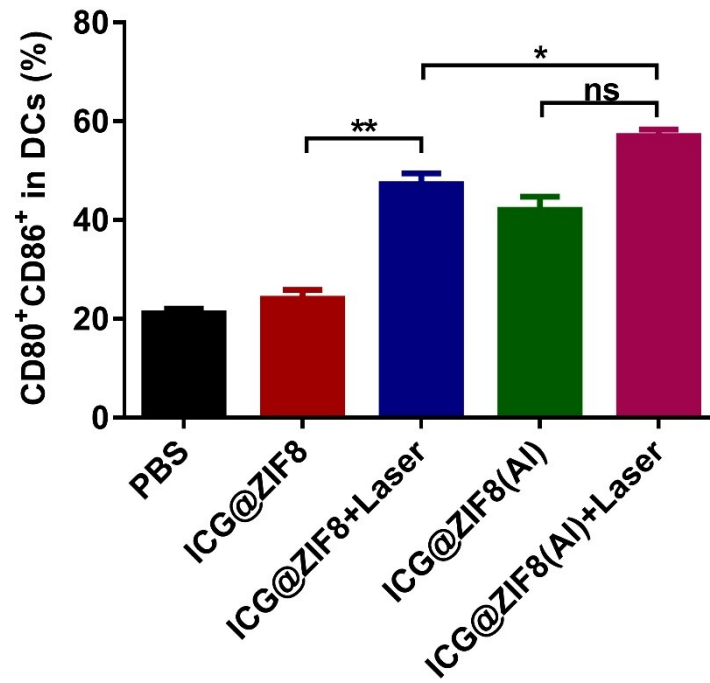


**Figure S8.** Expression of CD80 and CD86 on BMDCs induced by different formulation-treated 4T1 cells. Data are represented as the means  $\pm$  SD (n=3). \* $P < 0.05$ , \*\* $P < 0.01$ .

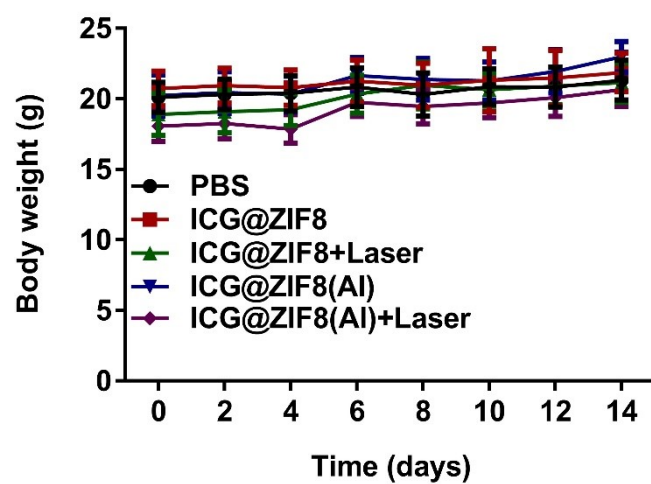


**Figure S9.** Body weight changes of mice after different treatments over 14 days.

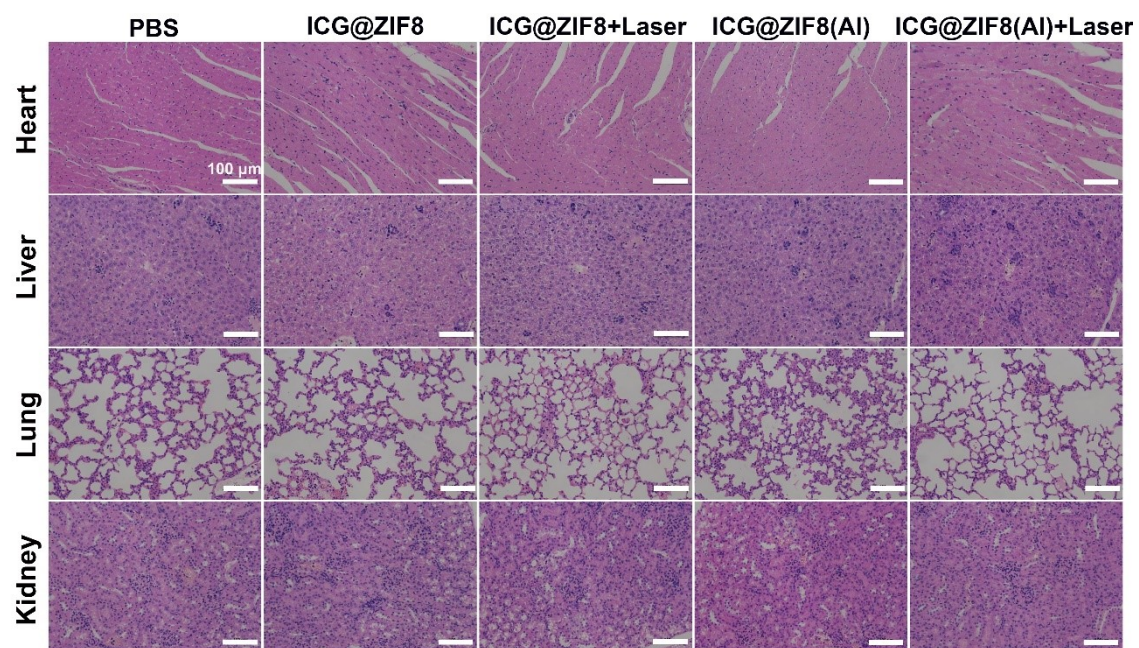


**Figure S10.** H&E staining images of major organs from mice after different treatments. Scale bars are 100 μm.

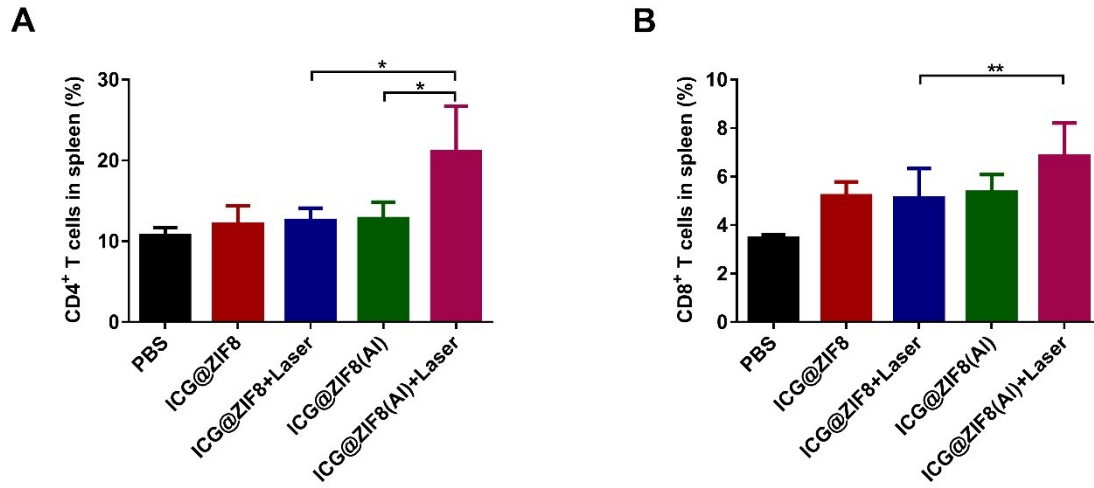


**Figure S11.** The CD3<sup>+</sup>CD4<sup>+</sup> (A) and CD3<sup>+</sup>CD8<sup>+</sup> (B) T cells in spleen harvested from mice treated with different formulations. Data are represented as the means  $\pm$  SD (n=6). \* $P < 0.05$ , \*\* $P < 0.01$ .

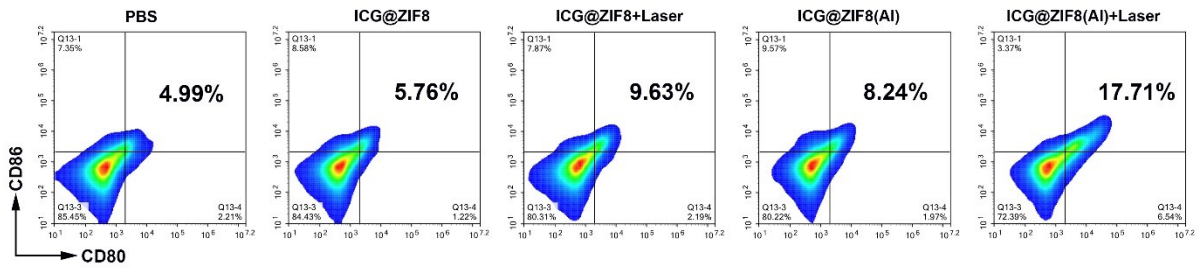


**Figure S12.** Flow cytometry analysis of DC maturation in the tumor-draining LNs.

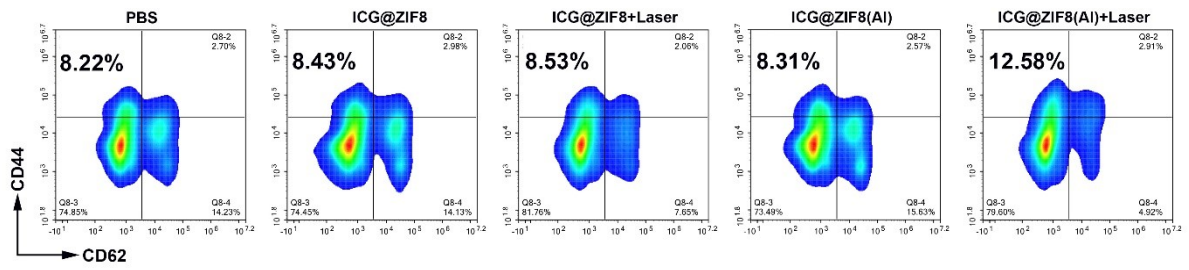
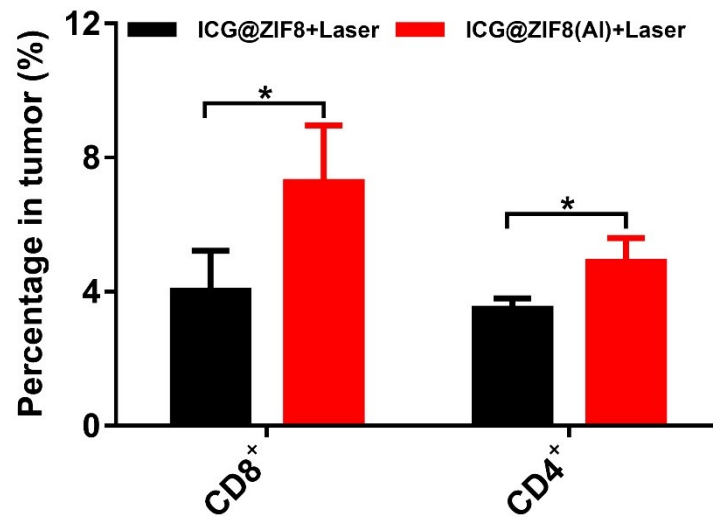
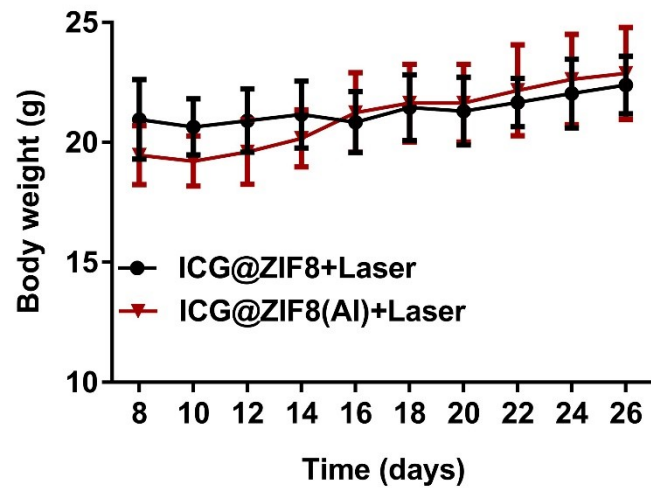


Figure S13. Representative graphs of effector memory T cells (CD44<sup>+</sup>CD62L<sup>-</sup>) in CD8<sup>+</sup> T cells.



**Figure S14.** The CD3<sup>+</sup>CD4<sup>+</sup> (A) and CD3<sup>+</sup>CD8<sup>+</sup> (B) T cells in the secondary tumor harvested from mice after different treatments. Data are represented as the means  $\pm$  SD (n=6). \* $P < 0.05$ .



**Figure S15.** Changes to mice body weight during various treatments.